

Light-Weight Cross-Modal Enhancement Method with Benchmark Construction for UAV-based Open-Vocabulary Object Detection

Zhenhai Weng¹, Xinjie Li¹, Can Wu¹, Weijie He¹, Jianfeng Lv², Dong Zhou^{3,4}, Zhongliang Yu^{1,✉},
✉ corresponding author

¹ School of Automation, Chongqing University

² School of Information Science and Engineering, Lanzhou University

³ Department of Control Science and Engineering, Harbin Institute of Technology

⁴ Department of Mechanical and Automation Engineering, The Chinese University of Hong Kong

Abstract

Open-Vocabulary Object Detection (OVD) faces severe performance degradation when applied to UAV imagery due to the domain gap from ground-level datasets. To address this challenge, we propose a complete UAV-oriented solution that combines both dataset construction and model innovation. First, we design a refined UAV-Label Engine, which efficiently resolves annotation redundancy, inconsistency, and ambiguity, enabling the generation of large-scale UAV datasets. Based on this engine, we construct two new benchmarks: UAVDE-2M, with over 2.4M instances across 1,800+ categories, and UAVCAP-15K, providing rich image-text pairs for vision-language pretraining. Second, we introduce the Cross-Attention Gated Enhancement (CAGE) module, a lightweight dual-path fusion design that integrates cross-attention, adaptive gating, and global FiLM modulation for robust text-vision alignment. By embedding CAGE into the YOLO-World-v2 framework, our method achieves significant gains in both accuracy and efficiency, notably improving zero-shot detection on VisDrone by +5.3 mAP while reducing parameters and GFLOPs, and demonstrating strong cross-domain generalization on SIMD. Extensive experiments and real-world UAV deployment confirm the effectiveness and practicality of our proposed solution for UAV-based OVD.

1. Introduction

Object detection, a fundamental task in computer vision, has witnessed rapid progress in recent years. However, traditional object detectors are limited to performing well only on object categories seen during training. This closed-set detection paradigm severely limits their application in open-world scenarios, particularly for agents like robots or UAVs. To address this limitation, researchers have in-

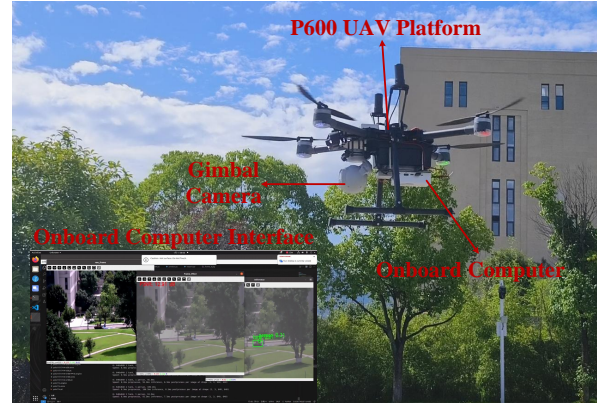


Figure 1. **Image of our UAV platform.** Our UAV experimental platform is equipped with a gimbal camera and an onboard computing device (NVIDIA ORIN NX 16G).

troduced open-vocabulary object detection (OVD)[24, 40]. By leveraging vision-language models (VLMs) such as CLIP[29] to align textual and visual information, OVD methods can detect novel categories not present in the training set, demonstrating remarkable zero-shot capabilities. Nevertheless, prior OVD models often rely on computationally intensive backbones or detectors with a large number of parameters, making them difficult to deploy on resource-constrained mobile platforms like robots and UAVs. In response to this challenge, real-time OVD methods have recently emerged[7, 36]. These methods strike a balance between high detection accuracy and real-time performance, enabling deployment on edge computing devices.

However, although existing real-time OVD methods perform well on natural-world images datasets(e.g. LVIS[12], COCO[21]), their performance on UAV-view object detection benchmarks(e.g. VisDrone[43], DroneVehicle[34]) is relatively poor, shown in Figure 2 and Figure 3. Several

factors likely account for this discrepancy. First, compared with conventional natural-image scenes, UAV imagery generally contains more cluttered backgrounds and objects that occupy far fewer pixels. Moreover, current open-vocabulary object detectors are trained almost exclusively on large-scale natural-world images datasets(e.g. Objects365[32], GoldG[18]), and this domain mismatch between training data and UAV views results in the pronounced drop in performance.

Therefore, in this paper we are motivated to advance real-time OVD for UAV perspective images. To achieve this goal, first, we optimized the LAE-Label Engine[28] and proposed the UAV-Label Engine. The UAV-Label Engine improves annotation accuracy and not only generates object detection datasets but also produces caption datasets, which are widely used in open-vocabulary detection tasks. Next, we used the UAV-Label Engine to generate our UAVDE-2M dataset and UAVCAP-15K dataset. UAVDE-2M is a huge UAV’s view object detection dataset with over 3 million instance annotations and more than 1,800 object categories. UAVCAP-15K is a caption dataset containing over 10,000 image-text pairs. Both datasets’ images are sourced from publicly available UAV-view task datasets.

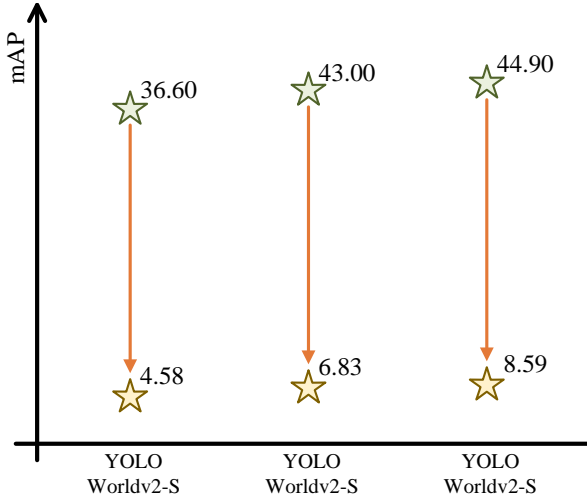


Figure 2. **Comparison of YOLO-World’s Zero-Shot Performance on the COCO and VisDrone Datasets.** The green stars demonstrate the mAP in COCO dataset, and the yellow ones demonstrate the mAP in VosDrone dataset. Specifically, for the VisDrone dataset, we use a confidence threshold of 0.001, a setting that is kept consistent across all following experiments.

To effectively embed textual guidance into UAV visual representations, we propose the cross-attention gated enhancement(CAGE) fusion module. The module’s innovation lies in a dual-path architecture that leverages a cross-attention governed by an gate mechanism to ensure precise, spatially-aware semantic grounding, while a parallel FiLM

layer provides global feature modulation, with both pathways integrated into the visual stream via a residual connection for robust enhancement.

Finally, to validate the practical efficacy of our model and dataset in real-world UAV applications, we deployed the trained model onto our custom UAV experimental platform and conducted a series of object detection experiments. We Figure 1 illustrates the UAV platform.

We summarize the main contributions as follows,

- We introduce two large-scale UAV-view datasets, UAVDE-2M and UAVCAP-15K, to facilitate the pre-training of open-vocabulary object detection models.
- We propose CAGE, a lightweight dual-path gated cross-attention fusion module, and integrate it into the YOLO-Worldv2 model.
- We conduct comparative experiments on the VisDrone dataset and in real-world UAV scenarios, demonstrating that our proposed model outperforms existing real-time OVD methods.

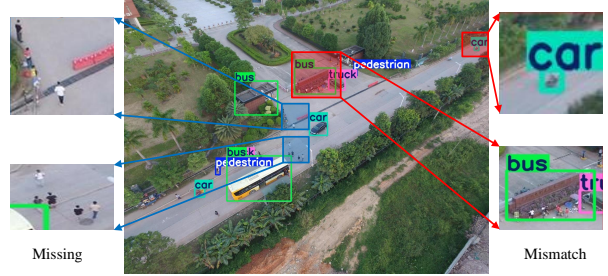


Figure 3. **Common Challenges in Open-Vocabulary Detection for UAV Imagery.** Common failure modes for OVD in aerial perspectives include false negatives (missed detections) and semantic mismatches.

2. Related Works

2.1. Open-Vocabulary Object Detection

OVD signifies a crucial evolution in computer vision, marking a departure from conventional closed-set paradigms toward a more flexible open-vocabulary framework. Pioneering research in this domain [40] was largely propelled by breakthroughs in vision-language models. These foundational methods employed pre-trained models, such as CLIP [29], to empower detectors with the ability to recognize object categories defined by free-form text during the inference phase. More contemporary approaches reframe OVD as an image-text matching task, leveraging large-scale image-text corpora to substantially broaden the model’s vocabulary. For instance, Grounding DINO [24] integrates grounded pre-training with detection transformers through cross-modal fusion mechanisms. However, a significant drawback of these models is their substantial computational

demand and architectural complexity, which precludes their use in real-time applications. In stark contrast, YOLO-World [7] is specifically engineered to address this challenge. By achieving a dramatic improvement in inference speed over traditional two-stage OVD methods, it effectively meets the latency requirements of practical scenarios. This advancement is accelerating the transition of OVD technology from academic exploration to industrial deployment, unlocking novel potentials in domains such as intelligent surveillance, robotic vision, and autonomous driving.

2.2. UAV-based Object Detection

UAV-based object detection(UAV-OD) presents unique challenges, particularly in detecting small objects and managing occlusions. The prevailing paradigms for UAV-OD fall into two categories: two-stage and single-stage. While two-stage detectors generally yield superior accuracy due to their more complex pipelines, their practical application is often limited by the need for deployment on resource-constrained airborne platforms. Therefore, single-stage methods have gained greater traction in the research community, as they provide a more favorable trade-off between sufficient accuracy and the high inference speeds required for real-time operation. Key research directions for improving single-stage detectors primarily involve leveraging finer-grained feature maps (e.g., P2)[10] for small object detection through multi-scale fusion[5, 6], formulating novel loss functions[22], and adopting high-resolution processing strategies such as image tiling with subsequent bounding box merging[23].

3. Datasets

Current object detection datasets captured from drone perspectives are insufficiently large in scale and lack diversity in object categories, making them unable to support the pretraining of OVD models. To address this limitation, this paper introduces the UAVDE-2M and UAVCAP-15K datasets, which fulfill the pretraining requirements for UAV-OVD.

3.1. UAVDE-2M

To construct an ultra-large-scale UAV-based OVD dataset, we introduce our UAV-Label Engine, by refining the existing LAE-Label Engine. The LAE-Label Engine simplistically categorizes existing remote sensing datasets into two types: Fully-annotated Datasets (FOD) and Completely Unlabeled Datasets (COD). For FOD, the engine directly slices the large-scale source images and then standardizes their format. For COD, it follows a sequential pipeline: it first employs the Segment Anything Model (SAM) to extract masks, then crops images based on these masks, uses a Large Vision-Language Model (LVM) to predict categories, and finally performs class filtering.

Building upon the LAE-Label Engine, our UAV-Label Engine introduces a more sophisticated data handling pipeline. Its core innovation is the classification of data into a new category named Partially-annotated Datasets (FOP) which alongside the standard FOD and COD. This FOP category is specifically designed to address datasets with valuable but not immediately usable annotations, tackling common challenges such as: 1) frame redundancy in UAV video data, 2) incompatible annotation types (e.g., segmentation vs. rotated boxes), and 3) ambiguous class labels (e.g., ‘vehicle,’ ‘obstacle’).

To address these challenges, we implement a targeted three-stage pipeline. For redundant images, we first extract deep features from the image sequence using DINOv2 and then compute the cosine similarity between adjacent frames. If the similarity exceeds a predefined threshold, the redundant frame is discarded. For inconsistent annotation formats, we develop custom scripts to convert all annotations into a standardized bounding box format. Finally, to resolve class ambiguity, we crop the object instances corresponding to ambiguous labels and perform a fine-grained re-classification to assign more specific categories via LVLM.

The UAVDE-2M dataset we proposed is composed of multiple collected datasets processed using the UAV-Label Engine. The details of each sub-dataset constituting UAVDE-2M are shown in Table 1. Word clouds illustrating the class distribution of the datasets shown in Figure 4. Our UAVDE-2M dataset covers over 2.4 million instances, more than 1800 categories, and a total of about 245K images. Moreover, UAVDE-2M includes not only ground targets from a UAV perspective but also water surface objects (e.g. SeaDronesSee[35], AFO[13]) and aerial objects (e.g. detfly[41]).

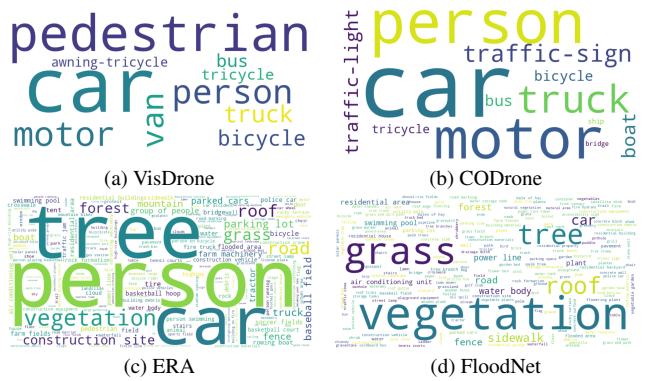


Figure 4. **Word clouds illustrating the class distribution of the datasets.** In contrast to the pre-annotated FOD datasets (e.g., (a), (b)), the COD datasets processed by our LVLM pipeline (e.g., (c), (d)) exhibit a significantly richer and more diverse set of class labels.

Table 1. **Detailed composition of the UAVDE-2M dataset.** Our UAVDE-2M dataset was constructed by sourcing and processing data from a diverse range of existing open-source datasets.

Datasets	Images	Instances	Categories
COF			
CARPK[17]	1448	89642	1
Cattle[9]	958	2079	1
LADD[33]	3112	5019	1
SeaDronesSee[35]	27042	60566	5
UAVASTE[20]	2432	3914	1
VisDrone[43]	8629	457066	10
Spanish Traffic[2]	14490	152594	3
CODrone[38]	50414	413750	12
DetFly[41]	10449	10449	1
FOP			
AeroScapes[27]	1110	8145	168
AFO[13]	1811	7128	6
auair[3]	1190	4666	8
DAC-SDC[37]	4547	4547	12
RescueNet[31]	20191	25500	88
uav123[26]	2091	12729	3
UAVDT-MOT[39]	637	10080	3
UAVOD10[14]	844	18334	10
UUD[4]	1164	20846	141
DroneVehicle[8]	27654	451618	5
ICG Drone Dataset	5121	35979	548
COD			
DenseUAV[8]	9096	156611	748
ERA[25]	2790	32879	838
FLAME3[16]	3766	51323	184
FloodNet[30]	11585	285180	772
SUES[44]	10829	32500	563
UAVDT-SOT[39]	1061	9029	304
University-1652[42]	21526	93282	643
Images: $\approx 245K$, Instance: $\approx 2.4M$, Categories: 1,853			

3.2. UAVCAP-15K

Compared to detection datasets, captioning datasets contain richer semantic information and are commonly used in conjunction with detection datasets during open-vocabulary detection (OVD) model pretraining. Datasets with detailed image captions significantly enhance the training of OVD models[11]. To construct a large-scale UAV-based caption dataset, we selected suitable images from the UAVDE-2M dataset and leveraged LVLM to generate image captions by integrating existing annotations. Specifically, we convert the absolute coordinates of objects in images into relative positional descriptions (e.g., top-left corner, bottom-right corner) and integrate them as part of the prompt. Simultaneously, the LVLM is required to maximize the description of object types, object actions, precise object locations, texts,

doublechecking relative positions between objects, etc[11]. Given the prevalence of small-sized objects in UAV perspective images, our prompts explicitly emphasize the detailed description of small-scale objects while deliberately minimizing the description of large-scale background elements. We used the Qwen2.5-VL[1] as the LVLM to construct UAVCAP-15K. The prompt and sample of UAVCAP-15K is shown in Figure 5.

4. Methods

4.1. Cross-Attention Gated Enhancement Module

To effectively integrate natural language guidance with visual features, we propose a novel fusion module, termed CAGE (Context-Aware Gated Ensemble). It enriches spatial image features with semantic context derived from textual descriptions. The module operates on an image feature map $F_{img} \in \mathbb{R}^{B \times H \times W \times C}$ and a sequence of text embeddings $F_{text} \in \mathbb{R}^{B \times N \times D}$, where D denotes batch size, H, W are spatial dimensions, C denotes channel depth, D denotes the number of categories, and D denotes the depth of the text embeddings. The module employs a multi-stage architecture combining: (1) a cross-modal attention mechanism, (2) a spatial context refinement block with an adaptive gate, (3) a global FiLM-based conditioning layer, and (4) a residual connection. The detailed structure of CAGE is shown in Figure 6.

The fusion process initiates by generating a spatial-semantic context map via multi-head cross-attention, where a query tensor, Q , is derived from the image features. The features are first projected by a 1×1 convolution, spatially flattened, and then normalized, a process which can be formulated as:

$$Q = LayerNorm(Flatten(Conv_{1 \times 1}(F_{img}))) \quad (1)$$

where P denotes the projection dimension. Currently, the key (K) and value (V) tensors are derived from the text features after layer normalization, followed by distinct linear transformations.

$$F'_{text} = LayerNorm(F_{text}) \quad (2)$$

$$\begin{aligned} K &= F'_{text} W_K \in \mathbb{R}^{B \times L \times P} \\ V &= F'_{text} W_V \in \mathbb{R}^{B \times L \times P} \end{aligned} \quad (3)$$

where W_K and W_V are the weight matrices of the linear projection layers. The attention scores are computed via scaled dot-product attention across h heads, each with dimension $d_k = P/h$. For the i -th head, the operation is:

$$head_i = softmax\left(\frac{Q_i K_i^T}{\sqrt{d_k}}\right) V_i \quad (4)$$



Caption: The image depicts a tranquil maritime scene featuring a single white boat cruising across calm, turquoise waters. A boat is positioned centrally in the lower middle portion of the frame, leaving a trail of white foam behind it as it moves forward. In the background, to the right, stands a distinctive architectural structure with a lattice-like design, partially obscured by the water's edge. The horizon stretches across the top of the image, meeting a clear sky that appears slightly hazy. The overall atmosphere is serene, with no other vessels or significant activity visible in the immediate vicinity.

Prompt: As an image understanding expert, observe this image and generate **one coherent paragraph** describing the scene naturally.

Requirements:

1. Mention ALL detected object categories and their counts (e.g., 'two people').
2. Describe relative positions (e.g., 'on the left', 'top-center') without coordinates.
3. Include the object types, textures and colors, object actions, precise object locations, texts, doublechecking relative positions between objects, etc.
4. Instead of describing the imaginary content, only describing the content one can determine confidently from the image.
5. Do not describe the contents by itemizing them in list form. Minimize aesthetic descriptions as much as possible.
6. Highlight micro-details of small objects.
7. Avoid summarizing backgrounds (sky/buildings) unless critically relevant.
8. Detected objects: {obj_list}

Structure guidance:

Start with scene context (time/location) → Core objects (position + count) → Notable details → Overall atmosphere.

Figure 5. **Prompt and a sample of UAVCAP-15K.** The UAVCAP-15K dataset utilizes a format of long-form, detailed descriptions for its captions. Moreover, it employs prompting techniques to enforce a consistent structure, ensuring all captions describe the image content in a uniform manner.

The outputs of all heads are concatenated and reshaped to form the context map $ctx_{map} \in \mathbb{R}^{B \times P \times H \times W}$.

In gated context refinement, the raw context map ctx_{map} undergoes a refinement and gating process to enhance local features. The context map is first projected to an intermediate channel dimension and then refined by a block \mathcal{F}_{dw} consisting of depthwise separable convolutions and GELU activations. An optional occlusion gate generates a per-pixel probability map $G \in [0, 1]^{B \times 1 \times H \times W}$ from the input image features, which determines the relevance of the textual context at each location, formulated as:

$$G = \sigma(\text{Conv}_{1 \times 1}(\text{GELU}(\text{Conv}_{3 \times 3}(F_{img})))) \quad (5)$$

where σ is the Sigmoid function. The refined context is then modulated by this gate:

$$ctx_{ref} = G \odot \mathcal{F}_{dw}(\text{Conv}_{1 \times 1}(ctx_{map})) \quad (6)$$

where \odot denotes element-wise multiplication.

The final stage integrates the refined context with the original image features using both concatenation and global modulation. The gated context $extctx_{extref}$ is concatenated with the original image features F_{img} along the channel dimension and subsequently fused via a convolutional block \mathcal{F}_{merge} to produce a pre-modulated feature map:

$$F_{pre-film} = \mathcal{F}_{merge}([F_{img}; ctx_{ref}]) \quad (7)$$

For global semantic control, a FiLM layer is utilized. The text features F_{text} are globally pooled to a sentence-level

vector f_{pool} . This vector is passed through a multi-layer perceptron \mathcal{F}_{film} to predict the channel-wise affine transformation parameters γ and β :

$$[\gamma, \beta] = \mathcal{F}_{film}(f_{pool}) \quad (\gamma, \beta \in \mathbb{R}^{B \times C_{out} \times 1 \times 1}) \quad (8)$$

The pre-modulated features are then transformed as follows:

$$F_{modulated} = (1 + \gamma) \odot F_{pre-film} + \beta \quad (9)$$

This operation allows the text command to scale and shift the visual feature activations dynamically.

To preserve the original visual information and ensure stable gradient flow, the module incorporates a parallel residual path, $F_{res} = \mathcal{F}_{res}(F_{img})$, where \mathcal{F}_{res} is either a 1×1 convolution or an identity map. The final output F_{out} is the sum of the residual path and the batch-normalized modulated features:

$$F_{out} = F_{res} + \text{BatchNorm}(F_{modulated}) \quad (10)$$

This design ensures that the fusion process enriches the visual features without catastrophically altering them, leading to a robust and effective fusion.

4.2. Module Integration Strategy

To seamlessly integrate the proposed CAGE module, we replace the T-CSPLayer blocks in the YOLO-World-v2 neck with our design. Each CAGE module receives multi-scale

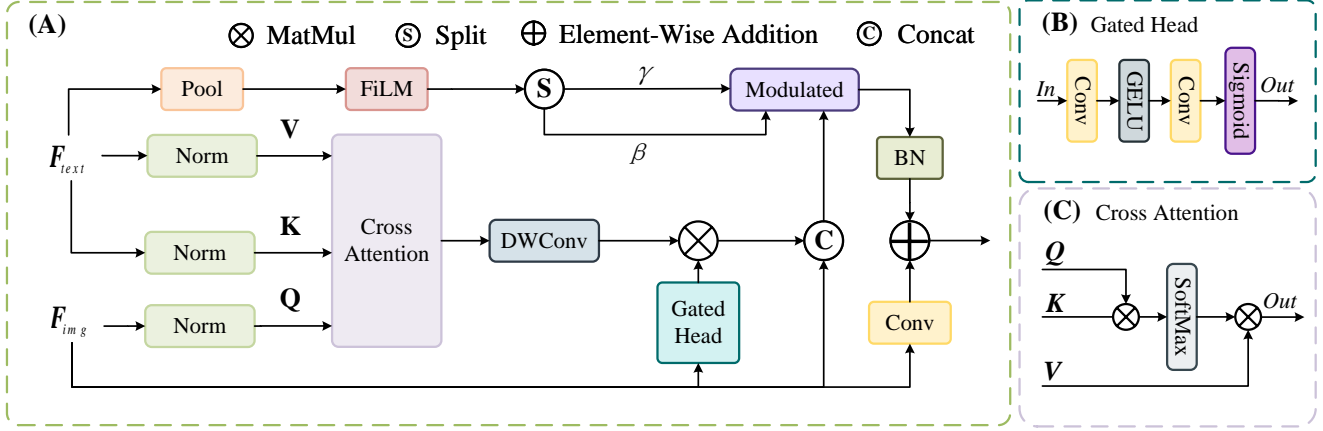


Figure 6. **Detail of cross-attention gated enhancement module.** The A is the overview of cross-attention gated enhancement module, B and C are the detail of gated head and cross attention respectively.

visual features from the PAN structure and text embeddings from the shared text encoder. The output dimensions are carefully aligned with those of the replaced T-CSPLayer, ensuring that the downstream architecture remains unchanged. This plug-and-play design allows CAGE to serve as a direct substitute for existing text–vision fusion modules without introducing additional architectural overhead.

4.3. Rationale and Advantages

Compared with the original T-CSPLayer, CAGE provides a more fine-grained and robust text–vision alignment. Its multi-head cross-attention enhances local semantic grounding, the occlusion-aware gating mechanism adaptively filters irrelevant context, and the global FiLM pathway modulates features at the channel level. These enhancements collectively yield richer cross-modal representations while preserving essential visual details through residual connections. By adopting a drop-in replacement strategy, CAGE not only improves detection accuracy but also demonstrates strong generalizability, making it easily transferable to other vision–language frameworks.

5. Experiments

5.1. Implementation details

Data. Following prior work[7, 36], we jointly pre-train our model on a combination of detection and captioning datasets, namely UAVDE-2M and UAVCAP-15K, where images from VisDrone[43] are excluded.

Training. All models we trained were processed for 100 epochs on a setup of $4 \times A800$ GPUs. We set the batch-size as 128, for data augmentation, we adopted the default strategy and parameters provided by Ultralytics[19].

Evaluation. During the evaluation phase, we employ a text-prompting approach. For each dataset, we utilize its class names directly as the text prompts.

5.2. Comparison Results

The zero-shot evaluation results of our proposed method on the VisDrone test set are presented in Table 2. The analysis first highlights the efficacy of domain-specific pre-training. Compared to the official YOLO-World-v2 models pre-trained on a general-purpose dataset (OGC), the models trained on our custom UAVDE-2M and UAVCAP-15K datasets exhibit substantial performance improvements. For instance, the mAP of the YOLO-World-v2-L model significantly increases from 8.59 to 12.2, which strongly demonstrates that our datasets can effectively enhance the model’s zero-shot generalization capability in aerial imagery scenarios. Furthermore, our proposed method demonstrates consistent superiority over the baselines under identical training conditions. Our models, outperform the original YOLO-World-v2 across all scales (S/M/L), achieving mAP scores of 10.0, 12.5, and 13.9, respectively, which are notable improvements over the baseline scores of 9.6, 11.1, and 12.2. In addition to its accuracy advantages, our method also excels in model efficiency. Taking the L-scale model as an example, ours boosts the mAP from 12.2 to 13.9 while simultaneously reducing the parameter count from 48M to 34M and GFLOPs from 204.5 to 144.0. This result underscores the ability of our method to significantly reduce model complexity and computational cost without sacrificing performance, making it highly suitable for resource-constrained edge computing applications. In summary, the experimental results thoroughly validate the dual effectiveness of our proposed datasets and method, achieving concurrent improvements in both accuracy and efficiency for the task of zero-shot object detection in UAV-based images.

Table 2. **Zero-shot Evaluation on VisDrone.** We evaluate our methods on VisDrone[43] test set in a zero-shot manner. For models trained on standard benchmark datasets, we adopt the weights released by Ultralytics[19]. OGC indicates Objects365[32], GoldG[18] and CC3M[7]. UAV indicates to UAVDE-2M and UAVCAP-15K.

Methods	Data	Size	Epochs	Params(M)	GFLOPs	AP50	mAP
YOLO-World-S	OGC	640	-	13	71.5	7.44	4.32
YOLO-World-M	OGC	640	-	29	131.4	10.9	6.64
YOLO-World-L	OGC	640	-	48	225.6	12.9	8.00
YOLO-World-v2-S	OGC	640	-	13	51.0	7.87	4.58
YOLO-World-v2-M	OGC	640	-	29	110.5	11.1	6.83
YOLO-World-v2-L	OGC	640	-	48	204.5	13.9	8.59
YOLO-World-v2-S	UAV	640	100	13	51.0	16.0	9.6
YOLO-World-v2-S w/ CAGE	UAV	640	100	11	46.6	16.4	10.0
YOLO-World-v2-M	UAV	640	100	29	110.5	17.7	11.1
YOLO-World-v2-M w/ CAGE	UAV	640	100	22	84.2	19.4	12.5
YOLO-World-v2-L	UAV	640	100	48	204.5	19.4	12.2
YOLO-World-v2-L w/ CAGE	UAV	640	100	34	144.0	21.2	13.9

To further validate the generalization capability of our curated datasets, we conducted a cross-domain zero-shot evaluation. Specifically, models pre-trained on our UAVDE-2M and UAVCAP-15K datasets were tested on the SIMD remote sensing dataset [15], whose image characteristics are related yet distinct from our UAV-based images. The results are presented in Table 3. The outcomes unequivocally demonstrate that pre-training on our datasets significantly enhances the model’s zero-shot performance in a novel domain. Compared to models trained on the general-purpose OGC dataset, the mAP of the YOLO-World-v2-L model trained on our datasets surged from 8.93 to 11.2, a substantial increase of 25.4%. This finding strongly suggests that our UAVDE-2M and UAVCAP-15K datasets enable the model to learn more generalizable visual representations that are not confined to UAV-specific scenarios but can be effectively transferred to broader remote sensing tasks. Furthermore, our proposed models also exhibit strong competitive performance in this cross-domain challenge. Our model surpasses its baseline with an mAP of 10.56, while our L-scale model achieves a highly competitive performance comparable to its baseline. In conclusion, this experiment fully substantiates the generalization value of our datasets, confirming that they equip the model with robust knowledge that transcends specific domain boundaries.

To dissect the specific contributions of our proposed datasets to the model’s performance, we conducted a series of ablation studies in VisDrone[43] test set, with the results detailed in Table 4. We established a YOLO-World-v2-S using a model pre-trained solely on the general-purpose OGC dataset, which achieved an mAP of only 4.58.

When we exclusively used our UAVDE-2M dataset for pre-training, the model’s performance experienced a sub-

Table 3. **Zero-shot Evaluation on SIMD.** We evaluate our methods on SIMD[15] test set, which is a remote sensing dataset different with uav-based images.

Methods	Data	AP50	mAP
YOLO-World-S	OGC	7.18	4.24
YOLO-World-M	OGC	9.98	5.79
YOLO-World-L	OGC	14.64	9.20
YOLO-World-v2-S	OGC	8.61	4.75
YOLO-World-v2-M	OGC	12.07	7.24
YOLO-World-v2-L	OGC	15.03	8.93
YOLO-World-v2-M	UAV	14.7	9.61
YOLO-World-v2-M w/ CAGE	UAV	15.9	10.56
YOLO-World-v2-L	UAV	16.9	11.2
YOLO-World-v2-L w/ CAGE	UAV	18.2	11.0

stantial leap, with the mAP soaring to 9.22. This dramatic improvement unequivocally demonstrates that the UAVDE-2M dataset provides the essential domain-specific knowledge required for effective zero-shot detection in UAV scenarios. Subsequently, by incorporating the UAVCAP-15K dataset for joint pre-training, the mAP was further boosted to 9.60. This indicates that UAVCAP-15K offers complementary and valuable information to UAVDE-2M, and their combination produces a synergistic effect that further enhances the model’s detection capabilities. In summary, this ablation study clearly validates our data curation strategy, confirming that UAVDE-2M serves as the foundational contributor to the performance gains, while UAVCAP-15K acts as a beneficial supplement, together yielding the optimal performance.

Table 4. **Ablation Study of pre-trained datasets.** We performed ablation experiments on the VisDrone[43] test set with different pre-trained data.

OGC	UAVDE-2M	UAVCAP-15K	AP50	mAP
✓			7.87	4.58
	✓		15.5	9.22
	✓	✓	16.0	9.60

Table 5. **Comparison of Inference Speeds on the NVIDIA Jetson Orin NX.** TensorRT models are benchmarked with FP16 precision, ONNX models are using CPU inference.

Methods \ Type	TensorRT(ms)	ONNX(ms)
YOLO8s-WorldV2	25.38	527
YOLOE-11s	28.34	591
YOLO8s-WorldV2 w/ CAGE	22.90	477

5.3. Real World Application

To validate the performance of our proposed model on the real-world UAV-based open-vocabulary object detection task, as well as its real-time operational capabilities on edge computing devices, we deployed our proposed model on an NVIDIA Jetson Orin NX 16G embedded computing device. This device was mounted on a P600 UAV, enabling the system to capture the video feed from the UAV’s gimbal camera, perform inference in real-time, and subsequently transmit the detection results back to a ground station via a video transmission module. Table 5 presents a comparison of the inference speeds between our proposed model and the baseline models on the NVIDIA Jetson Orin NX 16G. The results are shown in Figure 7. Our proposed method outperforms YOLO-World in terms of performance, as highlighted in the second column, our method demonstrates superior performance over YOLO-World-v2, particularly in challenging scenes with dense objects and heavy occlusion(e.g. parking lots).

6. Conclusion

In this work we address the long-standing domain gap that handicaps open-vocabulary object detection (OVD) once the viewpoint moves from ground to drone. First, we introduce UAVDE-2M and UAVCAP-15K currently the largest and most diverse UAV-specific datasets—covering 2.4 M instances across 1 853 categories and 15K richly-captioned images. A refined UAV-Label Engine automatically resolves redundancy, annotation inconsistency and class ambiguity, providing clean yet exhaustive annotations in hours rather than months. Second, we propose CAGE, a dual-path cross-attention gated enhancement module that fuses



Figure 7. **Visualization of open-vocabulary detection results from a real-world UAV perspective.** Our method demonstrates better detection performance.

language and vision with a controllable gate, global FiLM modulation and residual bypass. Plugged into YOLO-World-v2 with no other changes, CAGE yields:

- +5.3 mAP on VisDrone zero-shot ($8.59 \rightarrow 13.9$ for L-scale)
- −29 % parameters and −30 % GFLOPs, enabling 22.9ms latency on NVIDIA Jetson Orin NX
- +25.4 % mAP cross-domain on the SIMD remote-sensing benchmark

Ablation confirms that UAVDE-2M supplies the core domain knowledge and UAVCAP-15K provides complementary semantic supervision; together they are indispensable. Real-world flight tests further verify robust detection under varying altitude, illumination and weather. By open-sourcing the datasets, code and TensorRT models, we hope to accelerate the deployment of truly open-world, real-time perception systems on resource-constrained aerial platforms.

References

- [1] Shuai Bai, Keqin Chen, Xuejing Liu, Jialin Wang, Wenbin Ge, Sibao Song, Kai Dang, Peng Wang, Shijie Wang, Jun Tang, Humen Zhong, Yuanzhi Zhu, Mingkun Yang, Zhao-hai Li, Jianqiang Wan, Pengfei Wang, Wei Ding, Zheren Fu, Yiheng Xu, Jiabo Ye, Xi Zhang, Tianbao Xie, Zesen Cheng, Hang Zhang, Zhibo Yang, Haiyang Xu, and Junyang Lin. Qwen2.5-vl technical report. *arXiv preprint arXiv:2502.13923*, 2025. 4
- [2] Sergio Bemposta Rosende, Sergio Ghisler, Javier Fernández-Andrés, and Javier Sánchez-Soriano. Dataset: Traffic images captured from uavs for use in training machine vision algorithms for traffic management. *Data*, 7(5), 2022. 4
- [3] Ilker Bozcan and Erdal Kayacan. Au-air: A multi-modal unmanned aerial vehicle dataset for low altitude traffic surveillance. In *2020 IEEE International Conference on Robotics and Automation (ICRA)*, pages 8504–8510, 2020. 4
- [4] Yu Chen, Yao Wang, Peng Lu, Yisong Chen, and Guoping Wang. Large-scale structure from motion with semantic constraints of aerial images. In *Chinese Conference on Pattern Recognition and Computer Vision (PRCV)*, pages 347–359. Springer, 2018. 4
- [5] Yuming Chen, Xinbin Yuan, Jiabao Wang, Ruiqi Wu, Xiang Li, Qibin Hou, and Ming-Ming Cheng. YOLO-MS: Rethinking Multi-Scale Representation Learning for Real-time Object Detection. *IEEE Transactions on Pattern Analysis and Machine Intelligence*, pages 1–14, 2025. 3
- [6] Siyi Cheng, Jingnan Song, Mingliang Zhou, Xuekai Wei, Huayan Pu, Jun Luo, and Weijia Jia. Ef-detr: A lightweight transformer-based object detector with an encoder-free neck. *IEEE Transactions on Industrial Informatics*, 20(11):12994–13002, 2024. 3
- [7] Tianheng Cheng, Lin Song, Yixiao Ge, Wenyu Liu, Xinggang Wang, and Ying Shan. Yolo-world: Real-time open-vocabulary object detection. In *Proc. IEEE Conf. Computer Vision and Pattern Recognition (CVPR)*, 2024. 1, 3, 6, 7
- [8] Ming Dai, Enhui Zheng, Zhenhua Feng, Lei Qi, Jiedong Zhuang, and Wankou Yang. Vision-based uav self-positioning in low-altitude urban environments. *IEEE Transactions on Image Processing*, 33:493–508, 2024. 4
- [9] Fabricio de Lima Weber, Vanessa Aparecida de Moraes Weber, Pedro Henrique de Moraes, Edson Takashi Matsubara, Débora Maria Barroso Paiva, Marina de Nadai Bonin Gomes, Luiz Ocério Fialho de Oliveira, Sérgio Raposo de Medeiros, and Maria Istela Cagnin. Counting cattle in uav images using convolutional neural network. *Remote Sensing Applications: Society and Environment*, 29:100900, 2023. 4
- [10] Zewen Du, Zhenjiang Hu, Guiyu Zhao, Ying Jin, and Hongbin Ma. Cross-layer feature pyramid transformer for small object detection in aerial images. *IEEE Transactions on Geoscience and Remote Sensing*, 63:1–14, 2025. 3
- [11] Shenghao Fu, Qize Yang, Qijie Mo, Junkai Yan, Xihan Wei, Jingke Meng, Xiaohua Xie, and Wei-Shi Zheng. Llm-det: Learning strong open-vocabulary object detectors under the supervision of large language models. In *Proceedings of the Computer Vision and Pattern Recognition Conference (CVPR)*, pages 14987–14997, 2025. 4
- [12] Agrim Gupta, Piotr Dollar, and Ross Girshick. Lvis: A dataset for large vocabulary instance segmentation. In *Proceedings of the IEEE Conference on Computer Vision and Pattern Recognition*, 2019. 1
- [13] Jan Gąsienica-Józkowy, Mateusz Knapik, and Bogusław Cyganek. An ensemble deep learning method with optimized weights for drone-based water rescue and surveillance. *Integrated Computer-Aided Engineering*, pages 1–15, 2021. 3, 4
- [14] Wei Han, Jun Li, Sheng Wang, Yi Wang, Jining Yan, Runyu Fan, Xiaohan Zhang, and Lizhe Wang. A context-scale-aware detector and a new benchmark for remote sensing small weak object detection in unmanned aerial vehicle images. *Int. J. Appl. Earth Obs. Geoinformation*, 112:102966, 2022. 4
- [15] Muhammad Haroon, Muhammad Shahzad, and Muhammad Moazam Fraz. Multisized object detection using spaceborne optical imagery. *IEEE Journal of Selected Topics in Applied Earth Observations and Remote Sensing*, 13:3032–3046, 2020. 7
- [16] Bryce Hopkins, Leo O'Neill, Michael Marinaccio, Eric Rowell, Russell Parsons, Sarah Flanary, Irtija Nazim, Carl Seelstad, and Fatemeh Afghah. Flame 3 dataset: Unleashing the power of radiometric thermal uav imagery for wildfire management, 2024. 4
- [17] Meng-Ru Hsieh, Yen-Liang Lin, and Winston H. Hsu. Drone-based object counting by spatially regularized regional proposal networks. In *The IEEE International Conference on Computer Vision (ICCV)*. IEEE, 2017. 4
- [18] Aishwarya Kamath, Mannat Singh, Yann LeCun, Gabriel Synnaeve, Ishan Misra, and Nicolas Carion. Mdet - modulated detection for end-to-end multi-modal understanding. In *2021 IEEE/CVF International Conference on Computer Vision (ICCV)*, pages 1760–1770, 2021. 2, 7
- [19] Rahima Khanam and Muhammad Hussain. Yolov11: An overview of the key architectural enhancements, 2024. 6, 7
- [20] Marek Kraft, Mateusz Piechocki, Bartosz Ptak, and Krzysztof Walas. Autonomous, onboard vision-based trash and litter detection in low altitude aerial images collected by an unmanned aerial vehicle. *Remote Sensing*, 13(5), 2021. 4
- [21] Tsung-Yi Lin, Michael Maire, Serge Belongie, Lubomir Bourdev, Ross Girshick, James Hays, Pietro Perona, Deva Ramanan, C. Lawrence Zitnick, and Piotr Dollár. Microsoft coco: Common objects in context, 2015. 1
- [22] Tsung-Yi Lin, Priya Goyal, Ross Girshick, Kaiming He, and Piotr Dollár. Focal loss for dense object detection. In *2017 IEEE International Conference on Computer Vision (ICCV)*, pages 2999–3007, 2017. 3
- [23] Kai Liu, Zhihang Fu, Sheng Jin, Ze Chen, Fan Zhou, Rongxin Jiang, Yaowu Chen, and Jieping Ye. Esod: Efficient small object detection on high-resolution images. *IEEE Transactions on Image Processing*, 34:183–195, 2025. 3
- [24] Shilong Liu, Zhaoyang Zeng, Tianhe Ren, Feng Li, Hao Zhang, Jie Yang, Chunyuan Li, Jianwei Yang, Hang Su, Jun Zhu, et al. Grounding dino: Marrying dino with grounded pre-training for open-set object detection. *arXiv preprint arXiv:2303.05499*, 2023. 1, 2

- [25] Lichao Mou, Yuansheng Hua, Pu Jin, and Xiao Xiang Zhu. Era: A data set and deep learning benchmark for event recognition in aerial videos [software and data sets]. *IEEE Geoscience and Remote Sensing Magazine*, 8(4):125–133, 2020. 4
- [26] Smith Neil Mueller Matthias and Bernard Ghanem. A benchmark and simulator for uav tracking. In *Computer Vision – ECCV 2016*, pages 445–461, 2016. 4
- [27] Ishan Nigam, Chen Huang, and Deva Ramanan. Ensemble knowledge transfer for semantic segmentation. *2018 IEEE Winter Conference on Applications of Computer Vision (WACV)*, pages 1499–1508, 2018. 4
- [28] Jiancheng Pan, Yanxing Liu, Yuqian Fu, Muyuan Ma, Jiahao Li, Danda Pani Paudel, Luc Van Gool, and Xiaomeng Huang. Locate anything on earth: Advancing open-vocabulary object detection for remote sensing community. In *Proceedings of the AAAI Conference on Artificial Intelligence*, pages 6281–6289, 2025. 2
- [29] Alec Radford, Jong Wook Kim, Chris Hallacy, Aditya Ramesh, Gabriel Goh, Sandhini Agarwal, Girish Sastry, Amanda Askell, Pamela Mishkin, Jack Clark, Gretchen Krueger, and Ilya Sutskever. Learning transferable visual models from natural language supervision. In *Proceedings of the 38th International Conference on Machine Learning*, pages 8748–8763, 2021. 1, 2
- [30] Maryam Rahnemounfar, Tashnim Chowdhury, Argho Sarkar, Debvrat Varshney, Masoud Yari, and Robin Murphy. Floodnet: A high resolution aerial imagery dataset for post flood scene understanding. *arXiv preprint arXiv:2012.02951*, 2020. 4
- [31] Maryam Rahnemounfar, Tashnim Chowdhury, and Robin Murphy. Rescuenet: A high resolution uav semantic segmentation dataset for natural disaster damage assessment. *Scientific Data*, 10(1):913, 2023. 4
- [32] Shuai Shao, Zeming Li, Tianyuan Zhang, Chao Peng, Gang Yu, Jing Li, Xiangyu Zhang, and Jian Sun. Objects365: A large-scale, high-quality dataset for object detection. In *Proceedings of the IEEE/CVF International Conference on Computer Vision*, pages 8425–8434, 2019. 2, 7
- [33] Mikhail Shuranov, Denis Shurenkov, Dmitry Ruzhitsky, Victoria Martynova, Ekaterina Bykova, and Georgy Perevozchikov. Ladd: Lacmus drone dataset, 2023. 4
- [34] Yiming Sun, Bing Cao, Pengfei Zhu, and Qinghua Hu. Drone-based rgb-infrared cross-modality vehicle detection via uncertainty-aware learning. *IEEE Transactions on Circuits and Systems for Video Technology*, pages 1–1, 2022. 1
- [35] Leon Amadeus Varga, Benjamin Kiefer, Martin Messmer, and Andreas Zell. Seadronessee: A maritime benchmark for detecting humans in open water. In *Proceedings of the IEEE/CVF Winter Conference on Applications of Computer Vision*, pages 2260–2270, 2022. 3, 4
- [36] Ao Wang, Lihao Liu, Hui Chen, Zijia Lin, Jungong Han, and Guiguang Ding. Yoloe: Real-time seeing anything, 2025. 1, 6
- [37] Xiaowei Xu, Xinyi Zhang, Bei Yu, Xiaobo Sharon Hu, Christopher Rowen, Jingtong Hu, and Yiyu Shi. Dac-sdc: Design automation conference system design contest 2022 dataset, 2022. 4
- [38] Kai Ye, Haidi Tang, Bowen Liu, Pingyang Dai, Liujuan Cao, and Rongrong Ji. More clear, more flexible, more precise: A comprehensive oriented object detection benchmark for uav, 2025. 4
- [39] Hongyang Yu, Guorong Li, Weigang Zhang, Qingming Huang, Dawei Du, Qi Tian, and Nicu Sebe. The unmanned aerial vehicle benchmark: Object detection, tracking and baseline. *Int. J. Comput. Vision*, 128(5):1141–1159, 2020. 4
- [40] Alireza Zareian, Kevin Dela Rosa, Derek Hao Hu, and Shih-Fu Chang. Open-vocabulary object detection using captions. In *2021 IEEE/CVF Conference on Computer Vision and Pattern Recognition (CVPR)*, pages 14388–14397, 2021. 1, 2
- [41] Ye Zheng, Zhang Chen, Dailin Lv, Zhixing Li, Zhenzhong Lan, and Shiyu Zhao. Air-to-air visual detection of micro-uavs: An experimental evaluation of deep learning. *IEEE Robotics and Automation Letters*, 6(2):1020–1027, 2021. 3, 4
- [42] Zhedong Zheng, Yunchao Wei, and Yi Yang. University-1652: A multi-view multi-source benchmark for drone-based geo-localization. *ACM Multimedia*, 2020. 4
- [43] Pengfei Zhu, Longyin Wen, Dawei Du, Xiao Bian, Heng Fan, Qinghua Hu, and Haibin Ling. Detection and tracking meet drones challenge. *IEEE Transactions on Pattern Analysis and Machine Intelligence*, 44(11):7380–7399, 2021. 1, 4, 6, 7, 8
- [44] Runzhe Zhu, Ling Yin, Mingze Yang, Fei Wu, Yuncheng Yang, and Wenbo Hu. Sues-200: A multi-height multi-scene cross-view image benchmark across drone and satellite. *IEEE Transactions on Circuits and Systems for Video Technology*, 33(9):4825–4839, 2023. 4